


 Cite this: *Chem. Commun.*, 2020, 56, 5166

 Received 16th January 2020,
 Accepted 27th March 2020

DOI: 10.1039/d0cc00439a

rsc.li/chemcomm

Self-sacrificial MOFs for ultra-long controlled release of bisphosphonate anti-osteoporotic drugs†

 Maria Vassaki,^a Konstantinos E. Papathanasiou,^{ae} Chrystalleni Hadjicharalambous,^b Daphne Chandrinou,^a Petri Turhanen,^c Duane Choquesillo-Lazarte^{id}^d and Konstantinos D. Demadis^{id}*^a

In this paper we report drug delivery systems that are based on phosphonate MOFs. These employ biologically-acceptable metal ions (e.g. Ca²⁺ and Mg²⁺) and several anti-osteoporosis bisphosphonate drugs (etidronate, pamidronate, alendronate and neridronate), as the organic linkers. These materials have been synthesized, structurally characterized, and studied for the self-sacrificial release (by pH-driven dissolution) of the bisphosphonate active ingredient. They exhibit variable release rates and final % release, depending on the actual structure of the metal-bisphosphonate material. Their cytotoxicity profiles match those of the active ingredients.

Drug delivery systems (DDSS) have been devised in order to deliver active drug ingredients to specific target organs.¹ Among them, the controlled delivery systems (CDSs) can release the active drug in a designed and controlled fashion, keeping the therapeutic dosage constant.² The main reasons for the need of such systems are avoiding drug wastage, improved therapeutic results and control of undesirable side effects. CDSs function as controllers of the release of pharmaceuticals that have proven to be “problematic” because they are either unsuitably insoluble to biological fluids,³ or they are metabolized unacceptably rapidly.⁴

Osteoporosis is one of the most widespread bone-related conditions.⁵ It burdens millions of mostly elder patients compromising their quality of life. A widely accepted pharmaceutical treatment is based on bisphosphonates (BPs, a.k.a. “-dronates”).⁶

Historically, etidronate⁷ (a 1st generation drug) was introduced in 1977, followed by N-containing BPs, such as pamidronate, alendronate (2nd generation drugs),⁸ and zoledronate and risedronate (3rd generation drugs).⁹ Studies with N-containing BPs have shown that they are taken up by mature osteoclasts and inhibit farnesyl pyrophosphatase synthase, an enzyme of the mevalonate pathway.¹⁰ BPs are used successfully even today, with commercial names such as didronel, aredia, fosamax, vovina, actonel, *etc.*¹¹ However, these BP drugs present a number of challenges including limited bioavailability,¹² variable cytotoxicity, and a plethora of side-effects, such as osteonecrosis of the jaw, hypocalcemia, esophageal cancer, ocular inflammation, atrial fibrillation, *etc.*¹³ Hence, physicians are obligated to increase drug intake in order to achieve the required therapeutic dosage. Hence, careful design and fabrication of “smart” BP controlled release systems should allow the predictable and controlled delivery of the active BP drug that will conform to the patient’s needs and idiosyncrasies.

A limited number of BP CDSs have been reported.^{14–24} Some are based on hydrogels,^{14,16} others on nanocomposites,^{14,17–19} and some on metal-drug compounds.^{20–24}

Among the battery of exciting properties of MOFs is their ability to act as hosts and store active pharmaceutical ingredients.²⁵ Herein, we report the synthesis, and characterization of several metal BP coordination compounds and the pH-induced, controlled release of the BP active drug *via* a controlled self-sacrificial, self-degradation process. These CDSs demonstrate several desirable features, such as ease of preparation (MOF synthesis and tablet fabrication), precise crystal structures of the metal-bisphosphonate MOF ingredient, ultra-long release times (up to 20 days), pH-dependent controlled release, ability to “fine-tune” the rate of release and the final % release.

Complete synthesis/characterization details, tablet fabrication protocols, tablet textural and elemental characterization are found in the ESI.† Hydrothermal syntheses under autogenous pressure were carried out using a parallel synthesis high-throughput (Fig. S1 in the ESI†). For the controlled release studies,

^a Crystal Engineering, Growth and Design Laboratory, Department of Chemistry, University of Crete, Heraklion, Crete, GR-71003, Greece. E-mail: demadis@uoc.gr

^b Biochemistry Laboratory, Department of Chemistry, University of Crete, Heraklion, Crete, GR-71003, Greece

^c University of Eastern Finland, School of Pharmacy, Biocenter Kuopio, P. O. Box 1627, FIN-70211, Kuopio, Finland

^d Laboratorio de Estudios Cristalográficos, IACT, CSIC-Universidad de Granada, Granada-18100, Spain

^e National University of Science and Technology MISiS, Moscow 119049, Russia

† Electronic supplementary information (ESI) available: Synthesis/characterization/structural details, additional BP drug release data, cell viability studies. CCDC 1898065 (Ca-NER), 1898069 (Mg-ALE) and 1898068 (Mg-NER). For ESI and crystallographic data in CIF or other electronic format see DOI: 10.1039/d0cc00439a



tablets with each CDS (containing the BP either in its “free” form or as a metal-BP compound) were prepared by rigorous mixing of the solid ingredients (CDS and three common excipients, cellulose, lactose and silica). The same protocol was followed in all experiments. The tablets were exposed to a low pH (1.3) aqueous solution, to mimic the human stomach acidity. Aliquots of the supernatant were withdrawn at regular time intervals, and were measured by ^1H NMR spectroscopy. Unique characteristic peaks of each BP were integrated against an internal standard [Na-(3-(trimethylsilyl)propionic)-2,2,2,3,3- d_5 , TSP]. BP release curves were constructed that correlate % BP release with time.

Ten structurally characterized BP and metal-BP CDSs were evaluated for their controlled release characteristics: ETID (free), PAM (free), ALE (free), NER (free), Ca-ETID, Ca-PAM, Ca-ALE, Ca-NER, Mg-ALE and Mg-NER. Biocompatible metal ions (Ca^{2+} and Mg^{2+}) were used for the synthesis of the coordination compounds. The structures of the BPs in the studied CDSs were either determined or taken from literature sources. The crystal structures of the acid forms of ETID- H_2O ,²⁶ PAM (anhydrous),²⁷ ALE- H_2O ,²⁸ and NER (anhydrous),²⁹ and those of Ca-ETID,³⁰ Ca-PAM,³¹ and Ca-ALE³² have been reported. Crystallographic details of the new Ca-NER, Mg-ALE and Mg-NER are provided in the ESI.† Various views of the structures Ca-NER, Mg-ALE and Mg-NER are shown in Fig. 1.

Several controlled release experiments were carried out with excellent reproducibility (Fig. S2 and S3 in the ESI†) in order to determine the factors governing BP release. First, tablets with the “free” BPs, ETID, PAM, ALE, and NER were tested as “controls”. Then, the metal-BP containing tables (Ca-ETID, Ca-PAM, Ca-ALE, Ca-NER, Mg-ALE and Mg-NER) were evaluated. Fig. 2 (upper) shows the % BP release curves for the first 240 hours and relevant initial rate and final release data are provided in Table 1. A first observation is that free ETID (with a non-polar $-\text{CH}_3$ as the R side chain) is released rapidly and almost quantitatively at the early stages. On the other hand, PAM, ALE and NER (all with a polar and longer aminoalkyl side chain) demonstrate much slower initial release rates.

In all studied metal-containing CDSs, coordination of the BP drug to Ca^{2+} substantially decreases both release rate and % final release (Fig. 2, upper). For example, the Ca-ETID CDS shows a 4-fold deceleration of the release rate (from $4.93 \mu\text{mol min}^{-1}$ for “free” ETID to $1.12 \mu\text{mol min}^{-1}$ for Ca-ETID), and an increase of the time to reach a release plateau by a factor of 38 (192 hours), compared to the “free” ETID (5 hours).

In the ALE-containing CDS, the Ca-ALE shows a drop in the initial release rate by a factor of 3 (from $0.75 \mu\text{mol min}^{-1}$ for “free” ALE to $0.26 \mu\text{mol min}^{-1}$ for Ca-ALE), and a reduction in the final % release by a factor of *ca.* two. The drug release from Ca-PAM is slower ($0.31 \mu\text{mol min}^{-1}$) compared to that for “free” PAM ($0.40 \mu\text{mol min}^{-1}$), and reaches half of the final % release, compared to the “free” PAM system. Finally, the Ca-NER system demonstrates some idiosyncrasies. It is the only Ca-containing CDS that shows faster release ($0.75 \mu\text{mol min}^{-1}$) than the “free” NER system ($0.47 \mu\text{mol min}^{-1}$). These phenomena will be discussed later.

Interestingly, replacement of Ca^{2+} with Mg^{2+} in the “ALE” system causes a structural transformation. Although Ca-ALE is

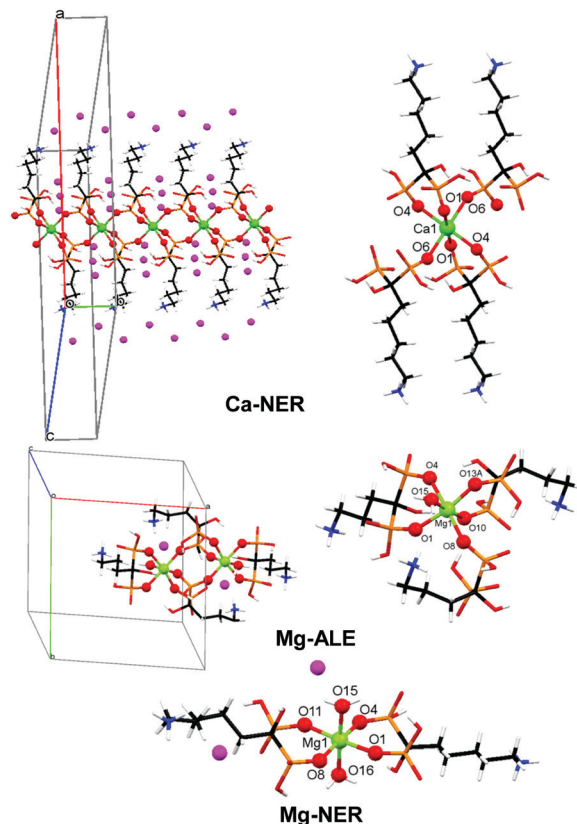


Fig. 1 Crystal views of the various CDSs used for controlled release. Color codes: metal centers, light green; P, orange, O, red; C, black; N, blue; H, white; lattice water, purple.

a 1D coordination polymer, Mg-ALE is a dinuclear complex (Fig. 1). Both metal centers remain octahedral, but Mg^{2+} contains a water ligand.

In any case, the controlled release characteristics of the Mg-ALE system are substantially altered compared to those of Ca-ALE (Table 1). The initial release rate observed for Mg-ALE is profoundly reduced (by nearly four times, $0.08 \mu\text{mol min}^{-1}$), compared to Ca-ALE ($0.26 \mu\text{mol min}^{-1}$), and almost ten times compared to “free” ALE ($0.75 \mu\text{mol min}^{-1}$). The final release of only 8% is reached after 192 hours. Similar observations can be noted for the Mg-NER CDS, which shows three times slower release ($0.22 \mu\text{mol min}^{-1}$) than the Ca-NER system ($0.75 \mu\text{mol min}^{-1}$), with a 24% release, reached after 192 hours (Table 1). Notably, replacement of Ca^{2+} with Mg^{2+} in the “NER” system also causes a disruption of the coordination polymer architecture and produces a Mg-NER mononuclear complex (Fig. 1).

It is noteworthy that none of the BP CDSs (either “free” or “metal-complexed”) reaches quantitative release (with the exception of “free” ETID and Ca-ETID) during the first plateau. Hence, it is important to address whether the equilibrium reached is final, and whether the remaining BP in the tablet can be quantitatively delivered. Therefore, step-wise release experiments were designed and carried out, in which the supernatant acidic fluid was replaced with “fresh”, low-pH aqueous medium after each release plateau was reached. These results for the Ca-NER, Ca-ALE, Ca-PAM, Mg-NER and Mg-ALE CDSs are



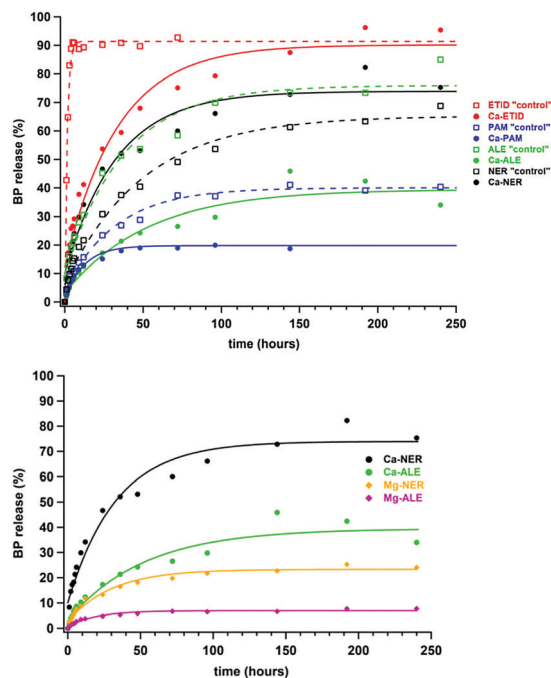


Fig. 2 Upper: Single-step controlled release of BPs (ETID, PAM, ALE, and NER) from CDSs containing the “free” BP drug (empty squares, dotted lines) and Ca-BPs (full circles, full lines). Lower: Comparison between Ca- and Mg-containing CDSs. Conditions: aqueous phase 50 mL, pH = 1.3, total tablet weight = 1.000 g.

Table 1 Release data for all studied CDSs

Controlled delivery system	Drug mass ^d (mg)	Initial rate ^b ($\mu\text{mol min}^{-1}$)	Release after 1st step (%)	Release after 2nd step (%)	Time required for 1st plateau (hours)
Free ETID	190	4.93	92	^c	5
Ca-ETID	261	1.12	96	^c	192
Free ALE	227	0.75	73	83	144
Ca-ALE	228	0.26	34	64	240
Free PAM	200	0.40	40	70	144
Ca-PAM	231	0.31	20	38	96
Free NER	236	0.47	63	90	192
Ca-NER	275	0.75	73	90	192
Mg-ALE	237	0.08	8	15	192
Mg-NER	276	0.22	24	49	192

^a Total tablet weight = 1.000 g (excipients included). ^b Based on the initial linear portion of the curve. ^c Not determined due to almost quantitative % release.

shown in Fig. 3. They strongly support the conclusion that after equilibrium is “reset”, BP release continues with the same kinetic features. For certain CDSs the step-wise release eventually reaches a final, essentially quantitative value (see ESI,† Fig. S4 and S5).

The differences noted in the release profiles for either the “free” or metal-complexed CDSs can be rationalized by carefully analyzing and comparing their crystal structures. Among the “free” BP systems, ETID and ALE are crystallized as monohydrates, whereas PAM and NER are anhydrous (Fig. S6–S9 in ESI†). Notably, ETID and ALE show the fastest release rates. It appears that the lattice water enhances drug release, possibly by facilitating drug hydration and/or disruption of hydrogen bonds. In addition the total number of hydrogen bonds in the structures of

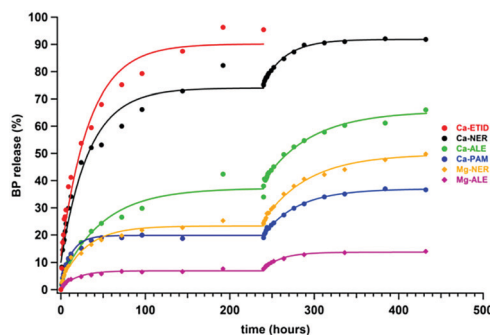


Fig. 3 Two-step sustained controlled release of BPs from metal-BP CDSs for 480 hours. Conditions are the same as in Fig. 2.

“free” BPs certainly impacts structure stability, and consequently, release rates. The faster-releasing systems display the lower number of unique hydrogen bonds, 5 for ETID and 12 for ALE, whereas the slower-releasing systems possess higher number of them, 14 for NER and 15 for PAM (Table S3 and Fig. S10–S24 in ESI†).

Differences are observed in the release profiles of the metal-BP CDSs. Again, the presence of lattice water seems to enhance release. For example, among the aminoalkyl Ca-BPs (all having the same 6-coordinated Ca^{2+} center), the ranking in the initial rate is Ca-ALE (0 lattice waters) < Ca-PAM (2 lattice waters) < Ca-NER (3 lattice waters). This scenario is perhaps dominant and in the unique case of the anhydrous “free” NER and trihydrate Ca-NER CDSs can explain why the latter releases NER more rapidly than the “free” NER system.

The M–O phosphonate coordination bond also seems to play an important role in the release characteristics of the metal-BP CDSs. By comparing the M–O bond distances in the Ca- and Mg-containing compounds, it is obvious that the Mg–O distances (2.007–2.173 Å) are significantly shorter than the Ca–O (2.297–2.346 Å) ones.³³ Hence, it is reasonable to assume that their resistance to acid-induced hydrolytic BP ligand detachment is a consequence of the M–O bond strength, thereby causing a deceleration in drug release.

Our results showed that the BP drugs were well tolerated by the cells (NIH3T3 mouse embryonic cell line, which is the standard cell line of fibroblasts, see ESI,† Fig. S25–S28).³⁴ Changes in cell viability were drug-specific and influenced by dose and treatment time. Overall, the behavior of all six Ca-, or Mg-BP CDSs was similar to their “free” BP counterparts (Fig. 4). Significant differences in cell viability were not observed between these formulations at any dose or duration of treatment tested. An exception was treatment with Ca-PAM, which decreased cell viability compared to treatment with PAM (approx. 20% vs. 80% relative to control), but this effect was observed only at the 10 μM dose and after 3 days. In comparison to the control, cultures treated with metal-NER and metal-ETID or “free” drugs, displayed similar cell viability at all time points and concentrations. Significant impact was observed following a 3 day treatment with ALE or PAM drugs at doses 10 μM and 100 μM respectively, which reduced cell viability to <10%, irrespective of drug modification.

These preliminary results open several possibilities in the exploitation of metal-BP MOFs as low-toxicity, controlled release



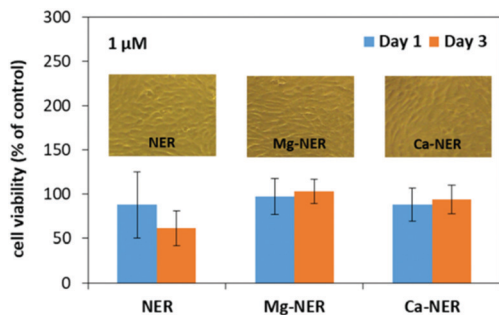


Fig. 4 Neridronate drug effects on cell viability of NIH3T3 cells after 1 and 3 days of treatment. At each time point data are expressed as % cell viability based on control cultures without drug treatment (100%). Each bar represents the mean \pm SE of triplicate samples from three independent experiments ($n = 9$). Inset pictures are optical microscopy images of NIH3T3 cells after 3 days of treatment.

systems for anti-osteoporosis medications, further expanding the applications of MOFs in the medicinal field.³⁵

KDD thanks the Hellenic Foundation for Research and Innovation (HFRI) under the HFRI PhD Fellowship (to MV, Fellowship Number 258). KEP gratefully acknowledges the financial support of the Ministry of Science and Higher Education of the Russian Federation in the framework of Increase Competitiveness Program of NUST «MISiS» (No. K4-2019-017), implemented by a governmental decree dated 16th of March 2013, N 211. Finally, we thank Professors D. Ghanotakis and G. Tsiotis (Department of Chemistry, University of Crete) for supporting the cell viability experiments with the necessary equipment.

Conflicts of interest

There are no conflicts to declare.

Notes and references

- 1 A. Mitra, C. H. Lee and K. Cheng, *Advanced Drug Delivery*, Wiley, New York, 2013.
- 2 F. Rossi, G. Perale and M. Masi, *Controlled drug delivery systems: Towards new frontiers in patient care*, PoliMI Springer Briefs, Heidelberg, 2016.
- 3 S. Kalepu and V. Nekkanti, *Acta Pharm. Sin. B*, 2015, **5**, 442.
- 4 G. M. Shenfield, *Clin. Biochem. Rev.*, 2004, **25**, 203.
- 5 U.S. Department of Health and Human Services. Bone health and osteoporosis: A report of the Surgeon General, Rockville, MD, 2004.

- 6 R. L. Hilderbrand, *The role of phosphonates in living systems*, CRC Press, 1983.
- 7 A. Ioachimescu and A. Licata, *Curr. Osteoporosis Rep.*, 2007, **5**, 165.
- 8 A. Grey and I. R. Reid, *Ther. Clin. Risk Manage.*, 2006, **2**, 77.
- 9 S. Pourgonabadi, S. H. Mousavi, Z. Tayarani-Najaran and A. Ghorbani, *Can. J. Physiol. Pharmacol.*, 2018, **96**, 137.
- 10 R. G. G. Russell, P. I. Croucher and M. J. Rogers, *Osteoporosis Int.*, 1999, **9**(Suppl. 2), S66–S80.
- 11 L.-A. Fraser, J. M. Albaum, M. Tadrous, A. M. Burden, S. Z. Shariff and S. M. Cadarette, *CMAJ Open*, 2015, **3**, E91.
- 12 H. Fleisch, *Endocr. Rev.*, 1998, **19**, 80.
- 13 N. B. Watts and D. L. Diab, *J. Clin. Endocrinol. Metab.*, 2010, **95**, 1555.
- 14 K. E. Papathanasiou, P. Turhanen, S. I. Brückner, E. Brunner and K. D. Demadis, *Sci. Rep.*, 2017, **7**, 4743.
- 15 F. Balas, M. Manzano, P. Horcajada and M. Vallet-Regí, *J. Am. Chem. Soc.*, 2006, **128**, 8116.
- 16 K. Zhang, S. Lin, Q. Feng, C. Dong, Y. Yang, G. Li and L. Bian, *Acta Biomater.*, 2017, **64**, 389.
- 17 W. Li, X. Xin, S. Jing, X. Zhang, K. Chen, D. Chen and H. Hu, *J. Mater. Chem. B*, 2017, **5**, 1601.
- 18 G. Golomb, M. Dixon, M. S. Smith, F. J. Schoen and R. J. Levy, *J. Pharm. Sci.*, 1987, **76**, 271.
- 19 X. Li, Y. W. Naguib and Z. Cui, *Int. J. Pharm.*, 2017, **526**, 69.
- 20 H. Epstein, V. Berger, I. Levi, G. Eisenberg, N. Koroukhov, J. Gao and G. Golomb, *J. Controlled Release*, 2007, **117**, 322.
- 21 B. Demoro, S. Rostán, M. Moncada, Z. H. Li, R. Docampo, C. Olea Azar, J. D. Maya, J. Torres, D. Gambino and L. Otero, *J. Biol. Inorg. Chem.*, 2018, **23**, 303.
- 22 D. Liu, C. He, C. Poon and W. Lin, *J. Mater. Chem. B*, 2014, **2**, 8249.
- 23 D. Liu, S. A. Kramer, R. C. Huxford-Phillips, S. Wang, J. D. Rocca and W. Lin, *Chem. Commun.*, 2012, **48**, 2668.
- 24 F. N. Shi, J. C. Almeida, L. A. Helguero, M. H. Fernandes, J. C. Knowles and J. Rocha, *Inorg. Chem.*, 2015, **54**, 9929.
- 25 P. Horcajada, C. Serre, G. Maurin, N. A. Ramsahye, F. Balas, M. Vallet-Regí, M. Sebba, F. Taulelle and G. Férey, *J. Am. Chem. Soc.*, 2008, **130**, 6774.
- 26 V. A. Uchtman and R. A. Gloss, *J. Phys. Chem.*, 1972, **76**, 1298.
- 27 L. M. Shkol'nikova, S. S. Sotman and E. G. Afonin, *Kristallografiya*, 1990, **35**, 1442.
- 28 J. Ohanessian, D. Avenel, D. El Manouni and M. Benramdane, *Phosphorus, Sulfur Silicon Relat. Elem.*, 1997, **129**, 99.
- 29 V. M. Coiro and D. Lamba, *Acta Crystallogr., Sect. C: Cryst. Struct. Commun.*, 1989, **45**, 446.
- 30 F. Niekel and N. Stock, *Cryst. Growth Des.*, 2014, **14**, 599.
- 31 D. Fernandez, D. Vega and A. Goeta, *Acta Crystallogr., Sect. C: Cryst. Struct. Commun.*, 2002, **58**, m494.
- 32 D. Fernandez, D. Vega and A. Goeta, *Acta Crystallogr., Sect. C: Cryst. Struct. Commun.*, 2003, **59**, m543.
- 33 *Metal Phosphonate Chemistry: From Synthesis to Applications*, ed. A. Clearfield and K. D. Demadis, Royal Society of Chemistry, Cambridge, U.K., 2012.
- 34 C. Hadjicharalambous, V. I. Alexaki, K. Alpantaki and M. Chatzinikolaïdou, *J. Pharm. Pharmacol.*, 2016, **68**, 1403.
- 35 G. Lan, K. Ni and W. Lin, *Coord. Chem. Rev.*, 2019, **379**, 65.

